

Computational analysis of concrete slabs subjected to perpendicular loads

Luiz E. G. de Mattos¹, Cosmo D. Santiago², Rodolfo K. Tessari³

Federal Technological University of Paraná (UTFPR), Apucarana-PR, Brasil.

¹ *luizmattosutfpr@gmail.com,* ² *cosmo@utfpr.edu.br,* ³ *rtessari@utfpr.edu.br.*

Abstract. The objective of the present paper is the analysis of the behaviour of concrete slabs when subjected to loads normal to the plane. The mathematical model is governed by the Lagrange's Equation in the two-dimensional plane. The differential equation is discretized by the Finite Difference Method in uniform grid with Neumann's boundary condition at the support positions. The system of algebraic equations is solved by the Gauss-Seidel method. Two case studies with distinct geometry, boundary conditions and loading are carried out. The first case is a simply supported triangular slab subject to uniformly distributed load. The second case simulates the hydrostatic loading on a reservoir wall or the earth thrust on a retaining wall. Through the computational analysis it was possible to capture displacements and internal forces (shear forces and bending moments) over the whole slab domain, which is crucial for designing such structural element. Numerical results also showed excellent agreement with analytical results extracted from the literature, validating the use of the proposed computational code.

Keywords: Slabs behaviour, Lagrange's Equation, Computational Analysis, Finite Difference Method.

1 Introduction

Slabs are present in the totality of buildings, because they allow the verticalization of the built space. According to Leitão and Castro [1], slabs are bi-dimensional laminar structures subject mainly to loading normal to their plane. These elements have the function of receiving the pavement loads and distributing them to support beams and columns.

Slabs are usually built of reinforced concrete and their design must prevent the occurrence of ultimate and serviceability limit states during the building's lifespan. In Brazil, the structural design of reinforced concrete slabs must follow the recommendations of the national standard, ABNT NBR 6118/2014 [2], which imposes the maximum allowed elongation presented by these elements. Excessive elongation can cause non-structural failures, like preventing the opening of doors and windows, as well as structural failures, provoking the opening of cracks and fissures that may cause the collapse of the element or the whole structure in worse scenarios.

Given the importance of properly describing the structural behaviour of slabs, researchers sought to relate it to physical laws and mathematical models. One of the most widespread and applied models combines the Theory of Elasticity with the Theory of Thin Plates or Kirchhoff's Plate Theory (Timoshenko and Woinowsky-Krieger [3]), which leads to a fourth order partial differential equation, called in-homogeneous bi-harmonic equation, or Lagrange's Equation (Szilard [4]).

The objective of this work is, therefore, to implement a computational code able to simulate the behaviour of slabs with different boundary conditions and subjected to perpendicular loads. Due to the complexity and non-linearity of the Lagrange's Equation, the Finite Difference Method (DFM) is used (Reddy and Gera [5]) with second order precision for the mathematical approximation of the partial derivatives. The resulting system of equations are solved by the Gauss-Seidel method.

2 Mathematical Model

To do a complete analysis of the behaviour thin slabs it is necessary to relate the internal efforts (torsional moments $m_{x,x}$ and $m_{y,y}$; bending moments $m_{x,y}$ and $m_{y,x}$; and shear forces $v_{z,x}$ and $v_{z,y}$) to the slab's displacement field through the deformation compatibility conditions and the constitutive law of the material. For this, the

previous knowledge of the transverse displacement ω , and the plane rotations around the axes x and y , θ_x and θ_y , as claim Leitão and Castro [1]. Figure 1 below represents the variables that characterize the displacement field and the internal efforts field.

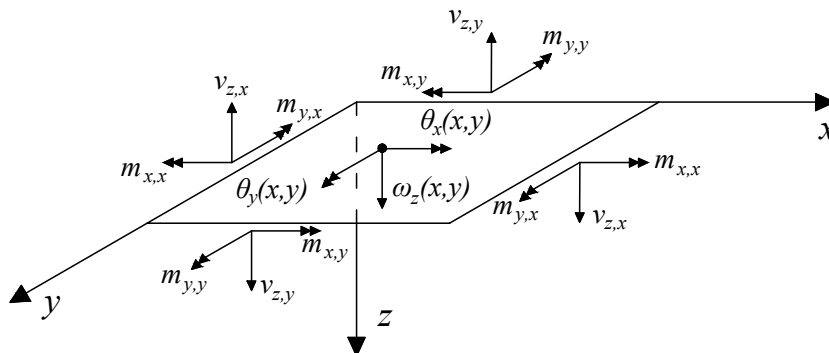


Figure 1. Balanced efforts and displacement fields of a thin slab

According to the classical Theory of Elasticity, the modulus of flexural rigidity of a slab with thickness h can be written as:

$$D = \frac{Eh^3}{12(1 - \nu^2)}, \tag{1}$$

being E and ν the Young’s modulus and the Poisson ratio of the material, respectively.

Szilar [4] states that it is possible to relate Kirchhoff’s Plate Theory with the Theory of Elasticity and compatible the fields of deformations, displacements, tensions and internal efforts of a slab. By doing this, the Lagrange’s differential Equation is obtained, which is the governing mathematical model for the slab’s deflection (ω) when subjected to perpendicular loads (q) on the plane (x, y) , given by

$$\frac{\partial^4 \omega}{\partial x^4} + 2 \frac{\partial^4 \omega}{\partial x^2 \partial y^2} + \frac{\partial^4 \omega}{\partial y^4} = \frac{q(x, y)}{D}, \tag{2}$$

so that the bending moments in the slab result:

$$m_x = -D \left(\frac{\partial^2 \omega}{\partial x^2} + \nu \frac{\partial^2 \omega}{\partial y^2} \right) \quad \text{e} \quad m_y = -D \left(\nu \frac{\partial^2 \omega}{\partial x^2} + \frac{\partial^2 \omega}{\partial y^2} \right). \tag{3}$$

3 Numerical Model

Analytical methods offer exact solutions for much mathematical models, however there is a great difficulty in its use to solve superior order partial differential equations, as is the case of Lagrange’s Equation. Therefore, numerical methods are much more appealing due to their capacity of representing the problem in a discrete form, using approximations and formulating models that can be solved by arithmetic operations. The Finite Difference Method (FDM) is based on the Taylor series expansion and consists of replacing derivatives by finite differences (Tannehill et al. [6]). This numerical method is widely used by the structural engineering scientific community, being used in this present work for the discretization of Eq. 2.

The FDM will be used to approximate the derivatives of a square domain that is discretized through a structured uniform grid. The grid consists of a plane belonging to the Cartesian space partitioned on a number of nodes (or points) given by $N = N_x N_y$, where N_x and N_y are the number of points in the directions x and y , respectively, including the plate contours. Each point of the computational grid is defined as $(x_i, y_j) = [(i - 1)\Delta x, (j - 1)\Delta y]$, with $i = 1, \dots, N_x$, $j = 1, \dots, N_y$, $\Delta x = L_x / (N_x - 1)$ and $\Delta y = L_y / (N_y - 1)$, where Δx and Δy are the elements size of the grid in the x and y directions, or the distance between two consecutive points.

An analogous way of representing the points on the computational stencil is associating the mesh indexes with cardinal points, as shown in Fig./ 2, where the point $P = (i, j)$ refers to the central point of the load/deflection.

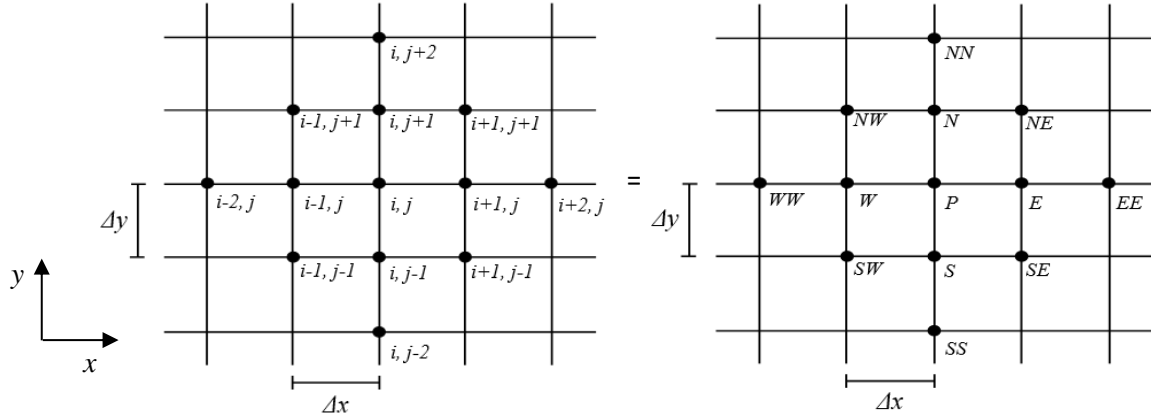


Figure 2. Computational stencil

3.1 Internal points discretization

Consider the domain of a plane slab discretized into a structured uniform grid. The partial derivative approximations of the Eq.2 by FDM (central differences) can be expressed as follow:

$$\left(\frac{\partial^4 \omega}{\partial x^4}\right)_{i,j} = \frac{(\omega_{i+2,j} - 4\omega_{i+1,j} + 6\omega_{i,j} - 4\omega_{i-1,j} + \omega_{i-2,j})}{\Delta x^4}, \quad (4)$$

$$\left(\frac{\partial^4 \omega}{\partial y^4}\right)_{i,j} = \frac{(\omega_{i,j+2} - 4\omega_{i,j+1} + 6\omega_{i,j} - 4\omega_{i,j-1} + \omega_{i,j-2})}{\Delta y^4}, \quad (5)$$

$$\left(\frac{\partial^4 \omega}{\partial x^2 \partial y^2}\right)_{i,j} = \frac{(\omega_{i+1,j-1} - 2\omega_{i+1,j} + \omega_{i+1,j+1} - 2\omega_{i,j-1} + 4\omega_{i,j} - 2\omega_{i,j+1} + \omega_{i-1,j-1} - 2\omega_{i-1,j} + \omega_{i-1,j+1})}{\Delta x^2 \Delta y^2}. \quad (6)$$

By replacing the derivatives approximations into Eq. 2, the resulting system of algebraic equations, we have the following system of algebraic equations with the number of unknowns equal to the number of deflections to be determined is given by:

$$A \cdot \mathbf{w} = \mathbf{b}, \quad (7)$$

where A is the matrix of derivative coefficients the Eqs.4 to 6, \mathbf{w} is the vector that accumulates the deflection values ω to be determined, and \mathbf{b} is the right-hand side. For vector the sake of brevity, the values of the coefficients and the right-hand side are not suppressed from this paper, but they can be found at Leitão and Castro [1].

Equation7 is solved using the iterative Gauss-Seidel method. The method consists in obtaining approximate solutions for the system of equations at each iterative step from a certain initial condition, \mathbf{w}_0 . The iterative process is stopped when $\|R^k\|_{\infty} / \|R^1\|_{\infty} \leq 10^{-6}$, where R^k is the residue of \mathbf{w} in iteration k (Fortuna [7]).

3.2 Boundary conditions

In real situations, a slab structure can present different support conditions at its edges, numerically called boundary conditions. These conditions can be geometrical (prescribed displacements or rotations), mechanical (prescribed efforts) or mixed, involving the previous two. Among the most utilized in civil construction are the boundary conditions of fixed edge, simply supported edge and free edge.

Simply supported edge. This condition prevents the deflection of the edge, ω , but allows its free rotation. Consequently, the bending moment, m , results zero in the support points, P . For this reason, it is considered a mixed boundary condition, being mathematically represented by the following expressions:

$$\omega_P = 0, \quad m_P = -D \left(\frac{\partial^2 \omega}{\partial x^2} + \nu \frac{\partial^2 \omega}{\partial y^2} \right) = 0. \quad (8)$$

Fixed edge. Different of the simply supported condition, the fixed edge not only prevents the point deflection, but also its rotation, θ . The boundary conditions are classified as geometrical, being expressed by:

$$\omega_P = 0, \quad \theta_P = \frac{\partial \omega}{\partial x} = 0. \quad (9)$$

Free edge. In the case of free edges, both deflection and rotation of the point are allowed. That way, the bending moment and the effective shear force, r , are also null (classified as a mechanical boundary condition):

$$m_P = -D \left(\frac{\partial^2 \omega}{\partial x^2} + \nu \frac{\partial^2 \omega}{\partial y^2} \right) = 0, \quad r_P = -D \left(\frac{\partial^3 \omega}{\partial x^3} + (2 - \nu) \frac{\partial^3 \omega}{\partial x \partial y^2} \right) = 0. \quad (10)$$

4 Case Studies

With the intention to presents the results obtained by the computational code developed in MATLAB, two case studies are analysed. The analysis simulate the behaviour of solid reinforced concrete slabs with a thickness of 10 cm, concrete resistance class C30, Young's modulus (E) equal to 31 GPa, and Poisson ratio (ν) of 0,2 (considering the use of granite as coarse aggregate), according to ABNT NBR 6118/2014 [2].

4.1 Case 1 - Simply supported triangular slab

The first case analysed is a triangular slab with simply supported edges subjected to an uniformly distributed load of 10 kN/m², as illustrated in Fig. 3.

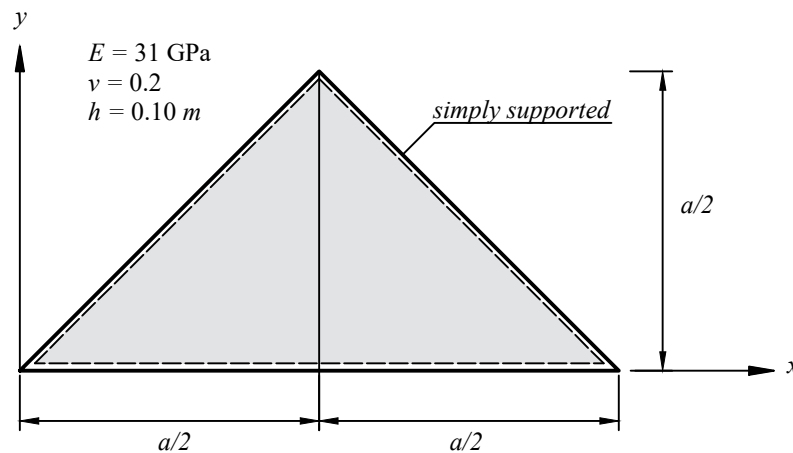


Figure 3. Triangular slab

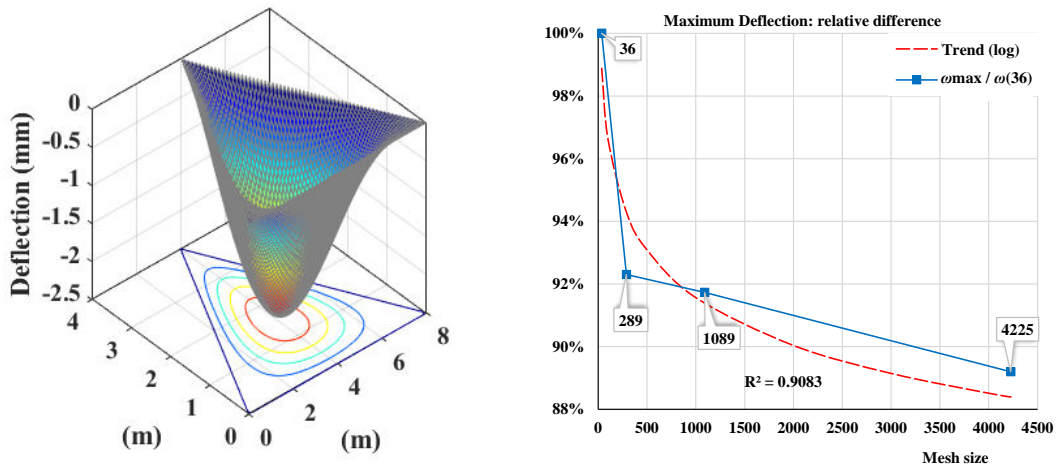
Table 1 presents the maximum deflection obtained for distinct values of slab length (a), with increasing mesh refinement. Szilard [4] reports the solution of this problem using a mesh with 36 nodal points.

Table 1. Maximum deflection of the slab ω_{max} (mm)

Lenght a (m)	Szilard [4]	36 points	289 points	1089 points	4225 points
1	0.0006666	0.0006666	0.0006153	0.0006115	0.0005946
2	0.0106664	0.0106664	0.0098458	0.0097844	0.0095146
4	0.1706630	0.1706631	0.1575334	0.1565504	0.1522330
8	2.7306081	2.7306089	2.5205344	2.5048061	2.43572898

Analysing the maximum deflection of the slab, results for the mesh with 36 points present an excellent agreement with those values found by values found by Szilard [4] (relative error of the order of 10^{-7} for $a = 8$ m). Results also show the impact of the mesh refinement: for a mesh with 4225 points (Fig. 4a), the maximum deflection is approximately 12% less in comparison to the less refined mesh. This difference increases as the mesh size grows, following a logarithmic trend (Fig. 4b).

Figure 4. Triangular slab deflections



(a) Slab deflection.

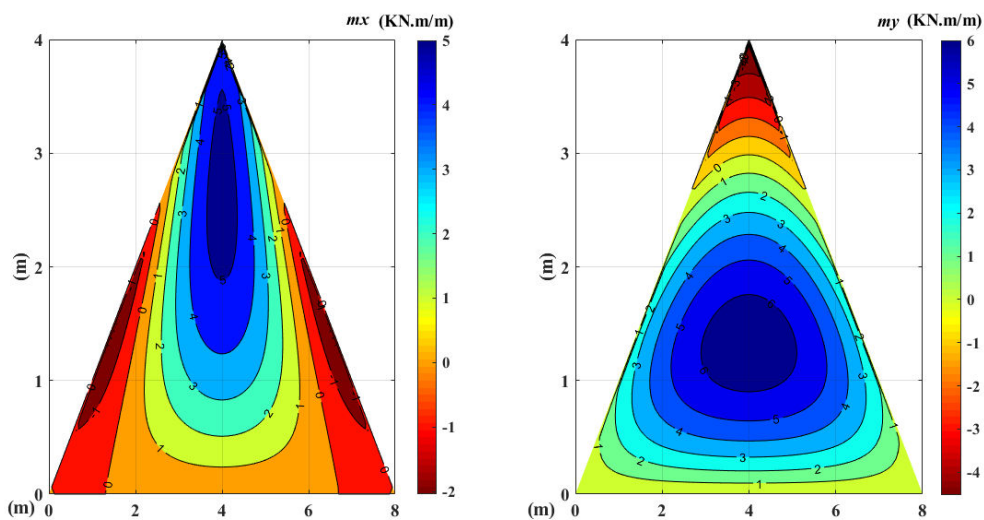
(b) Maximum deflection as a function of mesh refinement.

In addition to deflections, it is possible to estimate also the bending moments acting on x and y directions. The extreme values (most positive and most negative) found are presented in Tab. 2. Figure 5 illustrates the bending moments field in the x (left) and y (right) directions, respectively.

Table 2. Maximum (positive) and minimum (negative) bending moments in x and y directions

	Maximum (positive)	Minimum (negative)
m_x (KN.m/m)	5.4467	-2.0429
m_y (KN.m/m)	6.5864	-4.5305

Figure 5. Bending moments of the triangular slab



(a) Bending moments in x direction.

(b) Bending moments in y direction.

Through Fig. 5 we can observe that triangular slabs have the particularity of presenting negative bending moments in x and y directions. In simply supported rectangular slabs only positive bending moments are present.

It is worth mentioning that the bending moment in triangular slab's boundary is ever zero, due to the simply supported boundary condition.

4.2 Case 2 - Square slab with three fixed edges and one free edge (Hydrostatic loading - Earth thrust)

The second case study simulates the hydrostatic loading on a reservoir wall or the earth thrust on a retaining wall (Fig. 6). For the present analysis it was admitted the value of $q_o = 10 \text{ kN/m}^2$.

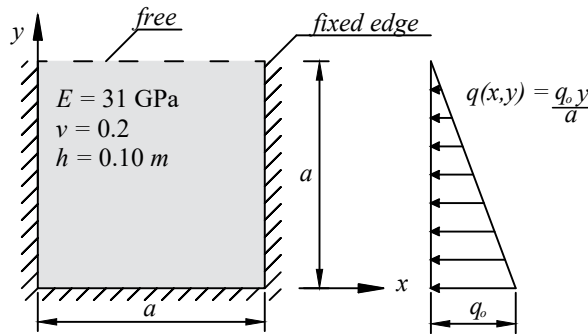


Figure 6. Square slab

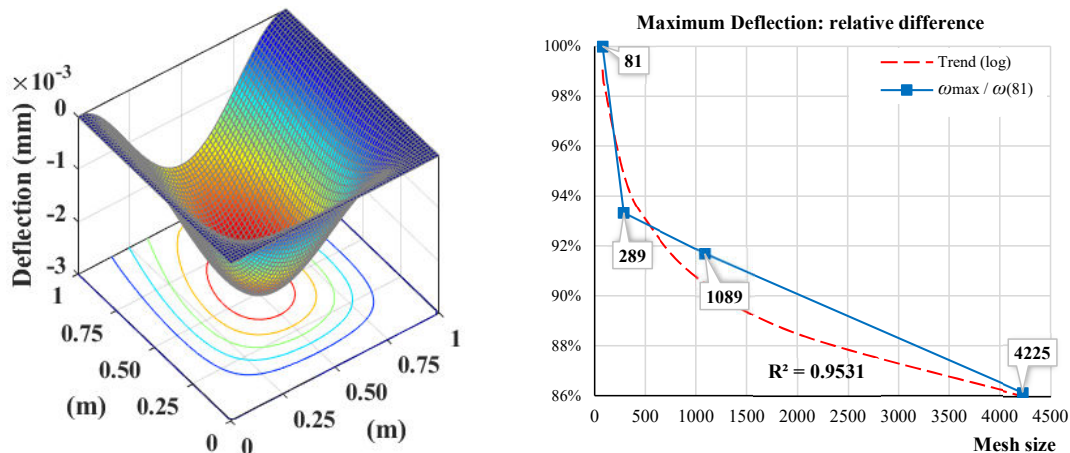
Table 3 presents the estimated deflection in the center of the slab and in the middle of the free edge, considering a length a of 1 meter and different mesh refinements. Results are compared to the analytical solution proposed by Timoshenko and Woinowsky-Krieger [3].

Table 3. Deflection of the square slab ω (mm)

Slab location (x, y)	Timoshenko <i>et al</i> [3]	81 points	289 points	1089 points	4225 points
(0.5 , 1.0)	0.0002415	0.0002259	0.0002108	0.0002071	0.0001946
(0.5 , 0.5)	0.0003605	0.0003335	0.0003065	0.0002994	0.0002922

Results show that the slab deflection decreases as the mesh refinement grows (more refined meshes generate lower deflection values), following, once again, a logarithmic trend (Fig. 7b). The deflection in the center of the slab simulated using a mesh with 4225 points (Fig. 7a) is 18.93% smaller then the solution proposed by Timoshenko and Woinowsky-Krieger [3] and 12.89% smaller then the less refined mesh. Another interesting issue is that the maximum deflection ($\omega_{max} = 2.938 \times 10^{-3}$) does not locate in the slab center, because the boundary condition does not present symmetry, as well as the linearly distributed loading has a gravity center displaced in relation to the central coordinate of the slab.

Figure 7. Square slab deflections



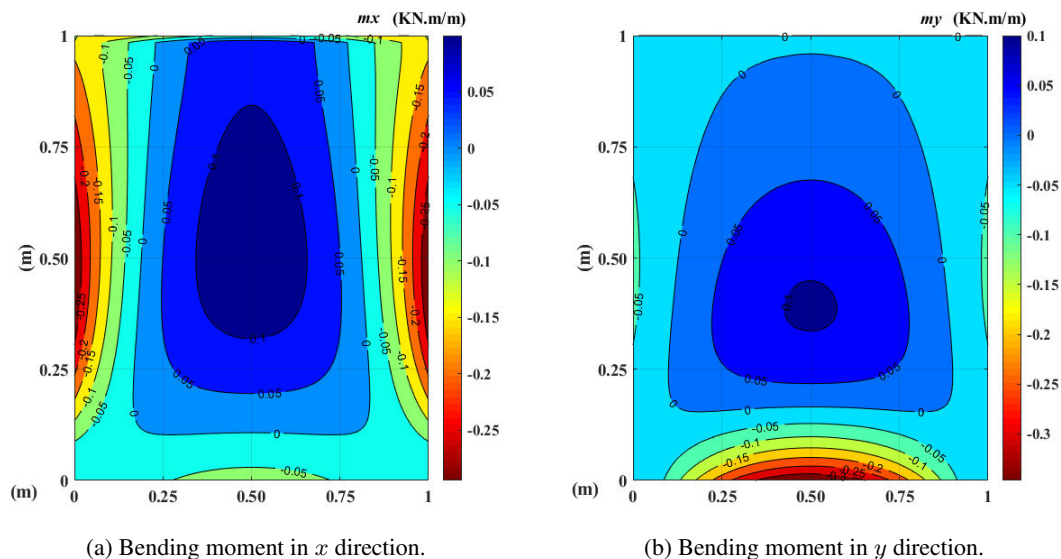
(a) Slab deflection.

(b) Maximum deflection as a function of mesh refinement.

Besides deflections, bending moments in the x and y directions of the slab, were also obtained, as shown in

Fig. 8. As expected, negative bending moments were found on the vicinity of the fixed edges, which are caused by the geometrical boundary conditions imposed by this type of support.

Figure 8. Bending moments of the square slab



5 Conclusions

In this present paper, a computational code was implemented to solve the Lagrange's Equation, in order to simulate the behaviour of slabs subjected to normal loads. The mathematical model was discretized by the Finite Difference Method and the system of algebraic equations was solved through the Gauss-Seidel method.

The first case study simulated a simply supported triangular slab subjected to uniform loading. As expected, the slab deflection varied according to the adopted dimensions. Larger span slabs presented greater deflections compared to shorter span slabs when subjected to the same uniform loading. The computer code developed generated similar results compared to Szilard [4], thus validating its use. It was also noted that meshes with a greater number of internal points provide better results. Besides deflections, bending moments on the triangular plate were also successfully captured by the implemented code.

The second case study simulates the hydrostatic loading on a reservoir wall or the earth thrust on a retaining wall. The deflection results in different mesh sizes are compared to the algebraic solution proposed by Timoshenko and Woinowsky-Krieger [3]. Again, more refined meshes held better results.

The case studies conducted proved the code to be effective in simulating the mechanical behaviour of concrete slabs, thus being of great help during structural design.

Authorship statement. The authors hereby confirm that they are the sole liable persons responsible for the authorship of this work, and that all material that has been herein included as part of the present paper is either the property (and authorship) of the authors, or has the permission of the owners to be included here.

References

- [1] Leitão, V. M. & Castro, L. M., 2014. Apontamentos sobre análise de lajes. *Elementos de estudo da disciplina Análise de Estruturas I: Instituto Superior Técnico*.
- [2] ABNT, N., 2014. 6118: Projeto de estruturas de concreto—procedimento. *Rio de Janeiro*.
- [3] Timoshenko, S. P. & Woinowsky-Krieger, S., 1959. *Theory of plates and shells*. McGraw-hill.
- [4] Szilard, R., 2004. Theories and applications of plate analysis: classical, numerical and engineering methods. *Appl. Mech. Rev.*, vol. 57, n. 6, pp. B32–B33.
- [5] Reddy, J. & Gera, R., 1979. An improved finite-difference analysis of bending of thin rectangular elastic plates. *Computers & Structures*, vol. 10, n. 3, pp. 431–438.
- [6] Tannehill, J. C., Anderson, D. A., & Pletcher, R. H., 1997. *Computational fluid mechanics and heat transfer*.
- [7] Fortuna, A. d. O., 2000. *Técnicas Computacionais para Dinâmica dos Fluidos Vol. 30*. Edusp.